Thomson scattering cross section in a magnetized, high-density plasma

A. F. A. Bott* and G. Gregori
Department of Physics, University of Oxford, Parks Road, Oxford OX1 3PU, United Kingdom

(Received 4 January 2019; revised manuscript received 27 May 2019; published 18 June 2019)

We calculate the Thomson scattering cross section in a nonrelativistic, magnetized, high-density plasma—in a regime where collective excitations can be described by magnetohydrodynamics. We show that, in addition to cyclotron resonances and an elastic peak, the cross section exhibits two pairs of peaks associated with slow and fast magnetosonic waves; by contrast, the cross section arising in pure hydrodynamics possesses just a single pair of Brillouin peaks. Both the position and the width of these magnetosonic-wave peaks depend on the ambient magnetic field and temperature, as well as transport and thermodynamic coefficients, and so can therefore serve as a diagnostic tool for plasma properties that are otherwise challenging to measure.

DOI: 10.1103/PhysRevE.99.063204

I. INTRODUCTION

Understanding radiation transport, opacity, and thermodynamic properties of strongly coupled, magnetized plasmas is important for modelling the atmosphere of magnetars and neutron stars [1], dynamo formation and evolution in planetary and stellar interiors [2,3], as well as inertial confinement fusion [4,5]. An important quantity that determines the opacity of these plasmas is the Thomson scattering cross section [1,6]. Moreover, while Thomson scattering of laser light is used as a plasma diagnostic tool [7], understanding the measurements in presence of a background magnetic field has, so far, been limited to special cases of negligible correlations between the electrons [1,8] or weakly coupled plasmas at wavelengths below the mean free path of constituent particles [9,10].

In this paper we will calculate the nonrelativistic Thomson scattering cross section associated with low-frequency collective excitations of a magnetized high-density plasma, under the assumption that such excitations can be described by magnetohydrodynamics (MHD). This approach allows a precise calculation of the effect of a magnetic field on the Thomson scattering cross section in a wide range of plasmas, including strongly coupled plasma—that is, plasma where the motion of charged particles is typically determined by both the presence of an ambient magnetic field, $\mathbf{B}_0$, and by short- and long-range correlations between all the particles in the system. We will show that the three-peak structure—one elastic peak and two Brillouin peaks—of the Thomson scattering cross section arising in an unmagnetized, high-density plasma becomes (in general) a five-peak structure when a finite ambient magnetic field is included. Physically, the appearance of an additional pair of peaks is associated with the existence of two distinct characteristic compressive excitations in magnetized plasma: the slow and fast magnetosonic modes. That such excitations are present in MHD is well known [11]; however, we believe this work is the first comprehensive calculation demonstrating their effect on the Thomson scattering cross section.

For our calculation to be valid, the wavelength of the light undergoing Thomson scattering must satisfy certain conditions: in particular, the light must be able to propagate through the plasma, while simultaneously having a large-enough wavelength for the MHD description to be appropriate. This constrains the type of plasma to which the calculated Thomson scattering cross section applies. The region of density-temperature phase space in which the calculation is applicable is shown in Fig. 1; furthermore, for a fixed temperature, Fig. 2 shows the dependence of the range of relevant photon energies on the electron density.

The structure of this paper is as follows. The double-differential Thomson scattering cross section is presented in Sec. II, and its relationship to the dynamic structure factor is discussed. We also explore the validity of the assumptions required for MHD to be an appropriate excitation model and justify the bounds on the relevant parameter spaces depicted in Figs. 1 and 2. In Sec. III, we write down the governing equations of MHD in a standard form and then derive evolution equations in terms of density, bulk fluid velocity, magnetic field, and temperature, as well as constitutive parameters of the matter. Section IV provides a derivation of the density autocorrelation function—and thereby the dynamic structure factor—arising in MHD for small-amplitude fluctuations. Before considering the general case in Sec. VII, we focus on the special cases of fluctuations whose wave vector is parallel to the magnetic field (Sec. V) and quasiperpendicular fluctuations (Sec. VI). Considering these particular cases—which can be treated analytically—allows for the clearest physical interpretation of the characteristic scattering peaks emerging in the MHD model for general fluctuations. Section VII also considers the case of fluctuations in dense plasmas where the magnetic energy density is only a finite fraction of the thermal energy density; this in turn anticipates how the dynamic structure factor might be altered from a purely hydrodynamic picture at sufficiently large magnetic field strengths. Finally, in Sec. VIII we briefly discuss how to extend our model to include quantum effects, and the model restrictions arising from their neglect.

*archie.bott@physics.ox.ac.uk

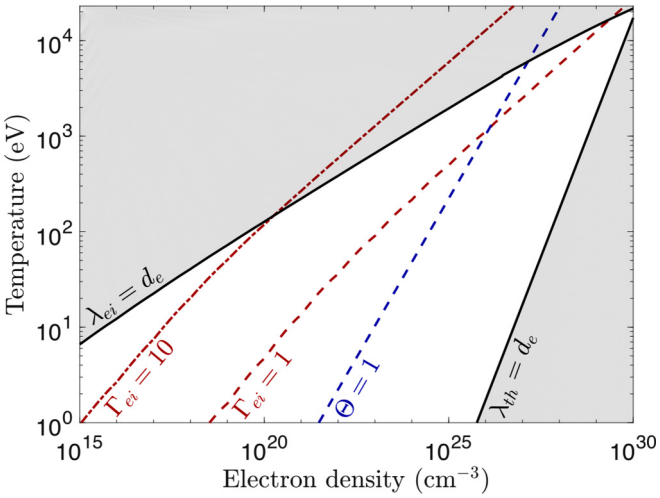

FIG. 1. Relevant region of density-temperature phase space for an aluminum plasma. Electron-densities and temperatures at which our calculations apply are depicted in white; other regions are in gray. Here λ_{ei} is the electron-ion mean free path, d_e the electron skin depth, and Γ_{ei} the electron-ion coupling parameter; these quantities are defined in Sec. II. The degeneracy parameter Θ and the thermal de Broglie wavelength λ_{th} are defined in Sec. VIII. Each equation listed on the figure defines a relationship between electron density and temperature. The origin of the relationships of d_e with λ_{ei} and λ_{th} are discussed in Sec. II and Sec. VIII, respectively. The ion charge of the aluminum plasma, which is itself a function of temperature, is approximated using a Thomas-Fermi model [12].

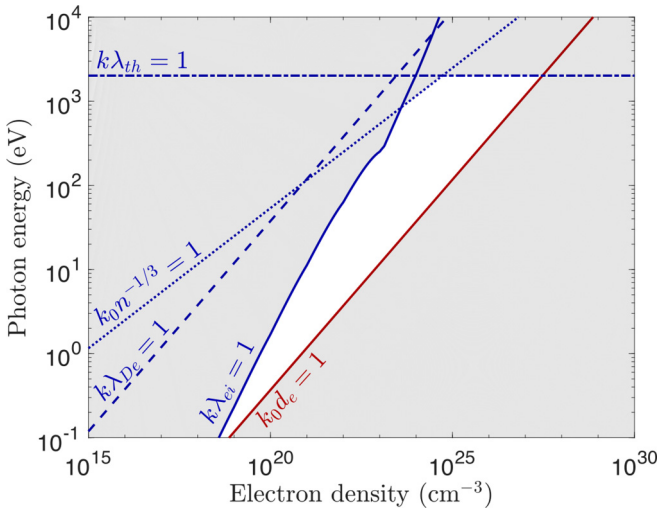

FIG. 2. Relevant photon-energy range (for varying electron number density). Photon energies at which the calculation applies are shown in white; other regions in gray. In this paper, k_0 is the wave number of the incident light to be Thomson scattered, and k is the magnitude of the scattering wave vector. The importance of the relationships $k\lambda_{De} = 1$, $k\lambda_{ei} = 1$, $k_0 d_e = 1$, and $k_0 n^{-1/3} = 1$ are discussed in Sec. II, while $k\lambda_{th} = 1$ is discussed in Sec. VIII. The assumed electron temperature was $T = 50$ eV, and the ion charge at a given density was again calculated using a Thomas-Fermi model.

II. THOMSON SCATTERING CROSS SECTION

Even neglecting particle correlations, calculating the scattering cross sections of photons by single electrons is a nontrivial task when there is a background magnetic field. This is because the motion of the electron under the influence of the incident electric field is altered by the presence of the background, introducing resonances at the cyclotron frequency [1]; thus the full polarization tensor, $\boldsymbol{\mathcal{P}}$, must be accounted for. Assuming that the ambient magnetic field is smaller than the Schwinger's field (thus neglecting vacuum polarization effects), we have that the differential cross section $d\sigma$ for Thomson scattering from a single (free) electron into a solid angle $d\Omega$ is

$$\frac{d\sigma}{d\Omega} = r_e^2 |\langle \hat{\boldsymbol{e}}^{(1)} | \boldsymbol{\mathcal{P}} | \hat{\boldsymbol{e}}^{(0)} \rangle|^2, \tag{1}$$

where $r_e = e^2/4\pi\epsilon_0 m_e c^2$ is the classical electron radius, and $\hat{\boldsymbol{e}}^{(0)}$ and $\hat{\boldsymbol{e}}^{(1)}$ are the incident and scattered photon polarization, respectively. Equation (1) can be simplified somewhat by noting that the polarization matrix is diagonal in the rotated frame where $\hat{\boldsymbol{e}}^{(0)} \equiv [\boldsymbol{e}_+^{(0)}, \boldsymbol{e}_-^{(0)}, \boldsymbol{e}_z^{(0)}]$, with $\boldsymbol{e}_z^{(0)}$ along the direction of $\mathbf{B}_0$ and $\boldsymbol{e}_\pm^{(0)} = \boldsymbol{e}_x^{(0)} \pm i\boldsymbol{e}_y^{(0)}$. A similar decomposition applies to the scattered photon polarization.

A further simplification applies if the velocity of the electron is much smaller than the speed of light (i.e., in the nonrelativistic regime). In this case, the polarization matrix is independent of the electron velocity, and we thus have [8,13,14]

$$\frac{d\sigma}{d\Omega} = r_e^2 \left| \frac{\langle \boldsymbol{e}_+^{(1)} | \boldsymbol{e}_+^{(0)} \rangle}{1 + \xi^{1/2} + i\gamma_R} + \frac{\langle \boldsymbol{e}_-^{(1)} | \boldsymbol{e}_-^{(0)} \rangle}{1 - \xi^{1/2} + i\gamma_R} + \frac{\langle \boldsymbol{e}_z^{(1)} | \boldsymbol{e}_z^{(0)} \rangle}{1 + i\gamma_R} \right|^2 \equiv r_e^2 |f_{(\hat{\boldsymbol{e}}^{(1)}, \hat{\boldsymbol{e}}^{(0)})}|^2, \tag{2}$$

where $\xi = (\omega_{ce}/\omega_0)^2$, with ω_0 the incident photon frequency, $\omega_{ce} = eB_0/m_e$ the electron cyclotron frequency, and $\gamma_R \omega_{ce}^2/\omega_0 = e^2\omega_{ce}^2/6\pi\epsilon_0 m_e c^3 \approx 4 \times 10^{15} (B_0/10^{12}\ \mathrm{G})^2\ \mathrm{s}^{-1}$ is the radiative damping coefficient. While the above expression uses a value for the background magnetic field that is typical for magnetars, the actual damping coefficient γ_R is independent of B_0. Equation (2) applies for $\omega_{pe}^2 \ll \omega_0^2$, where ω_{pe} is the plasma frequency. We see that the cross section is strongly enhanced at the cyclotron resonance, corresponding to the resonant photon absorption and reemission between Landau levels. This is an effect that is not present when there is no ambient magnetic field.

Since in the nonrelativistic limit the cross section is the same for all electrons, the quantity $f_{(\hat{\boldsymbol{e}}^{(1)}, \hat{\boldsymbol{e}}^{(0)})}$ plays the same role as a scattering form factor. We now consider a system consisting of many electrons in a high-density plasma. Because the plasma can sustain different type of waves, energy can be exchanged between the incident photons and the waves. The double-differential cross section then reads as [6]

$$\frac{d^2\sigma}{d\Omega d\omega_1} = N_e r_e^2 |f_{(\hat{\boldsymbol{e}}^{(1)}, \hat{\boldsymbol{e}}^{(0)})}|^2 \frac{\omega_1}{\omega_0} S_{ee}(\boldsymbol{k}, \omega), \tag{3}$$

where N_e is the total number of electrons, ω_1 the scattered photon frequency, $\omega = \omega_0 - \omega_1$, and $\boldsymbol{k} = \boldsymbol{k}_0 - \boldsymbol{k}_1$ (for $\boldsymbol{k}_0$ the incident wave vector and $\boldsymbol{k}_1$ the scattered wave vector). We note that the response of the system is anisotropic with respect

to the direction of the background magnetic field. The quantity $S_{ee}(\boldsymbol{k}, \omega)$, known as the dynamic structure factor, encodes the angular and energy distribution of the scattering that results from collective motions of the electrons, which in turn are functions of macroscopic plasma properties such as temperature and density. While the above expression applies to free electrons in the plasma, it can be generalized to the case of an electron-ion plasma [15–17]. Focusing on low-frequency excitations, the relevant part of the cross section reads as [16,17]

$$\frac{d^2\sigma}{d\Omega d\omega_1} = N r_e^2 |f_{(\hat{\boldsymbol{e}}^{(1)},\hat{\boldsymbol{e}}^{(0)})}|^2 \frac{\omega_1}{\omega_0} |f_I(k) + q(k)|^2 S_{nn}(k,\omega), \quad (4)$$

where N is the total number of ions, $f_I(k)$ is the ion form factor (accounting for the bound-electron correlations) and $q(k)$ is the screening cloud of kinematically bound free electrons that follow the ion. The dynamic structure factor $S_{nn}(\boldsymbol{k}, \omega)$ is defined by [17,18]

$$S_{nn}(\boldsymbol{k},\omega) = \frac{1}{2\pi N} \int dt\, e^{i\omega t} \langle n(\boldsymbol{k},t) n(-\boldsymbol{k},0)\rangle, \quad (5)$$

where $n(\boldsymbol{k}, t)$ is the Fourier component of the ion number density with wave vector $\boldsymbol{k}$ (wave number $k \equiv |\boldsymbol{k}|$) and fluctuation frequency ω. The operator $\langle ... \rangle$ corresponds to a thermal average over the particles' ensemble.

It is clear that knowledge of the dynamic structure factor is essential for a detailed derivation of the scattering spectrum incorporating collective excitations. For magnetized, high-density plasma, the model of those excitations we choose to employ to calculate the dynamic structure factor is that of MHD, accounting for viscosity, electrical resistivity, and heat conductivity. A fluid model of this sort is suitable for plasma whose characteristic mean free paths λ_{ei} and λ_{ii} of constituent electrons and ions, respectively, due to Coulomb collisions—defined for weakly coupled plasma by

$$\lambda_{ei} \equiv \frac{12\pi^{3/2} k_B^2 \epsilon_0^2 T_e^2}{Z e^4 n_e \log\Lambda}, \quad (6)$$

$$\lambda_{ii} \equiv \frac{12\pi^{3/2} k_B^2 \epsilon_0^2 T_i^2}{Z^3 e^4 n_e \log\Lambda}, \quad (7)$$

where ϵ_0 is the permittivity of free space, k_B the Boltzmann constant, $\log\Lambda$ the Coulomb logarithm, Z the ion charge, and T_e and T_i are the electron and ion temperatures, respectively [11]—are much smaller than the typical length scales k^{-1} associated with the fluctuations of interest. Noting that $\lambda_{ii} \sim \lambda_{ei}/Z^2 \lesssim \lambda_{ei}$ in a plasma with equilibrated electron and ion temperature $T \equiv T_i = T_e$, as well as $k = 2\omega_0 \cos\theta_T/c$ (where θ_T is the Thomson scattering angle), the requirement that $k\lambda_{ei} \ll 1$ places the following bound on the photon energy for which the MHD model is valid:

$$\hbar\omega_0 \ll 350 \left[\frac{\sec(\theta_T/60^\circ)}{2}\right] \left(\frac{\log\Lambda}{1.5}\right) \left(\frac{Z}{5.7}\right) \times \left(\frac{n_e}{10^{23}\ \mathrm{cm}^{-3}}\right) \left(\frac{T}{50\ \mathrm{eV}}\right)^{-2} \mathrm{eV}. \quad (8)$$

Here we have approximated the mean ion charge of the plasma using a Thomas-Fermi model [12]. Since the incident light must be able to propagate through through the plasma (that is, $\omega_0 \gg \omega_{pe}$), there also exists a lower bound on the photon energy in terms of the electron number density:

$$\hbar\omega_0 \gg 31 \left(\frac{n_e}{10^{23}\ \mathrm{cm}^{-3}}\right)^{1/2} \mathrm{eV}. \quad (9)$$

The simultaneous requirement that both these conditions be satisfied—that is, $\lambda_{ei} \ll d_e$, where $d_e \equiv c/\omega_{pe}$ is the electron plasma skin depth—leads to a constraint on the plasma density at a given temperature:

$$n_e \gg 1.3 \times 10^{20} \left[\frac{\sec(\theta_T/60^\circ)}{2}\right]^{-2} \left(\frac{\log\Lambda}{1.5}\right)^{-2} \times \left(\frac{Z}{5.7}\right)^{-2} \left(\frac{T}{50\ \mathrm{eV}}\right)^{4} \mathrm{eV}. \quad (10)$$

This constraint is shown in Fig. 1 and is the sense in which we refer to our calculation as applying only to "high-density" plasma. Provided densities are not so large as to introduce quantum effects (see Sec. VIII), we conclude that MHD is indeed the appropriate model for calculating the dynamic structure factor for magnetized plasma satisfying (10).

There exist further constraints on the photon energy to which our calculation applies. For excitations to be collective, it is necessary that $k\lambda_{De} \ll 1$ (where $\lambda_{De} \equiv \sqrt{\epsilon_0 k_B T/e^2 n_e}$ is the electron plasma Debye length); this implies the following upper bound on the photon energy:

$$\hbar\omega_0 \ll 1.2 \times 10^3 \left[\frac{\sec(\theta_T/60^\circ)}{2}\right] \times \left(\frac{n_e}{10^{23}\ \mathrm{cm}^{-3}}\right)^{1/2} \left(\frac{T}{50\ \mathrm{eV}}\right)^{-1/2} \mathrm{eV}. \quad (11)$$

Whether this condition is more or less restrictive than (8) depends on the electron-ion coupling parameter, defined by

$$\Gamma_{ei} \equiv \frac{Ze^2}{4\pi\epsilon_0 k_B T} \sqrt[3]{\frac{4\pi n_e}{3}}. \quad (12)$$

The electron mean-free path λ_{ei} and Debye length λ_{De} are then related by $\lambda_{De} = \Gamma_{ei}\lambda_{ei}$. For a plasma with weak electron-ion coupling ($\Gamma_{ei} \ll 1$), it follows that $\lambda_{ei} \gg \lambda_{De}$, and thus condition (8) is more restrictive. On the other hand, in a plasma with strong electron-ion coupling ($\Gamma_{ei} \gtrsim 1$), for which $\lambda_{ei} \lesssim \lambda_{De}$, all collective excitations must satisfy $k\lambda_{ei} \ll 1$. In addition to this constraint, the scattering wave number must be sufficiently small that many particles are sampled and subsequently ensemble averaged: in other words, $k_0 n^{-1/3} \ll 1$. In terms of photon energy, this gives

$$\hbar\omega_0 \ll 510 \left[\frac{\sec(\theta_T/60^\circ)}{2}\right] \left(\frac{Z}{5.7}\right)^{-1/3} \left(\frac{n_e}{10^{23}\ \mathrm{cm}^{-3}}\right)^{1/3} \mathrm{eV}. \quad (13)$$

These two constraints are illustrated in Fig. 2. We note that while in principle these constraints also lead to further restrictions on the electron-density–temperature parameter space to which our calculation applies, in practice the actual constraints are much less restrictive that either mean-free-path

constraint (10) or constraints arising from neglecting quantum effects (Sec. VIII).

For completeness, we observe that at high densities and with magnetic fields significantly below the critical value, Coulomb collisions can also alter the Thomson scattering cross section associated with noncollective excitations in strongly coupled plasma from that of classical weakly coupled plasma. More specifically, the deexcitation rate of the Landau levels and the radiative damping coefficient must be changed [14] to $\gamma_R \to \gamma_R + \gamma_{\rm coll}$, where

$$\frac{\gamma_{\rm coll}\omega_{ce}^2}{\omega_0} = 3.1\times 10^8\left(\frac{B_0}{10^{12}\ {\rm G}}\right)^{-3/2}\left(\frac{n_e}{10^{20}\ {\rm cm}^{-3}}\right)Z^2\ {\rm s}^{-1}. \tag{14}$$

Thus, in dense plasmas, collisional processes can significantly broaden the cyclotron resonances.

III. GENERAL EQUATIONS FOR MAGNETOHYDRODYNAMICS

We now focus on the calculation of $S_{nn}(\boldsymbol{k},\omega)$ in a magnetized plasma. The approach we use begins by writing down the relevant fluid equations and then applying a linearization procedure in order to derive the density fluctuations [19–23]. The governing equations of MHD are conservation laws of mass, momentum, magnetic flux, and internal energy:

$$\frac{d\rho}{dt} = -\rho\nabla\cdot\boldsymbol{u}, \tag{15a}$$

$$\rho\frac{d\boldsymbol{u}}{dt} = -\nabla p - \nabla\cdot\boldsymbol{\Pi} + \frac{(\nabla\times\boldsymbol{B})\times\boldsymbol{B}}{\mu_0}, \tag{15b}$$

$$\frac{d\boldsymbol{B}}{dt} = \boldsymbol{B}\cdot\nabla\boldsymbol{u} - \boldsymbol{B}\nabla\cdot\boldsymbol{u} - \nabla\times(\eta\nabla\times\boldsymbol{B}), \tag{15c}$$

$$\rho\frac{d\epsilon}{dt} = -p\nabla\cdot\boldsymbol{u} - \boldsymbol{\Pi}:\nabla\boldsymbol{u} + \eta\frac{|\nabla\times\boldsymbol{B}|^2}{\mu_0} - \nabla\cdot\boldsymbol{q}, \tag{15d}$$

where $\rho = Mn$ is the mass density (with M the ion mass), t is time, $\boldsymbol{u}$ the bulk fluid velocity,

$$\frac{d}{dt} \equiv \frac{\partial}{\partial t} + \boldsymbol{u}\cdot\nabla \tag{16}$$

the convective derivative, p the pressure, $\boldsymbol{\Pi}$ the viscosity tensor, $\boldsymbol{B}$ the magnetic field, μ_0 the permeability of free space, η the (assumed isotropic) resistivity, ϵ the internal energy, and $\boldsymbol{q}$ is the heat flux.

For subsequent calculations, it is helpful to rewrite the internal energy conservation law (15d) as an evolution equation for the fluid temperature T in terms of density, bulk flow velocity, and the magnetic field. We do this by using the first law of thermodynamics,

$$\frac{d\epsilon}{dt} = T\frac{d\mathcal{S}}{dt} + \frac{p}{\rho^2}\frac{d\rho}{dt}, \tag{17}$$

where $\mathcal{S}$ is the specific entropy, to write down a conservation law for specific entropy:

$$\rho T\frac{d\mathcal{S}}{dt} = -\boldsymbol{\Pi}:\nabla\boldsymbol{u} + \eta\frac{|\nabla\times\boldsymbol{B}|^2}{\mu_0} - \nabla\cdot\boldsymbol{q}. \tag{18}$$

In turn, it can be shown using thermodynamic identities (see Appendix A) that

$$\frac{d\mathcal{S}}{dt} = \frac{C_V}{T}\left(\frac{dT}{dt} - \frac{\gamma-1}{\alpha_T}\frac{d\rho}{dt}\right), \tag{19}$$

where C_V is the heat capacity at constant volume, γ the adiabatic index, and α_T the coefficient of thermal expansion. Thus, we deduce that the temperature evolves according to

$$\rho C_V\frac{dT}{dt} = -\frac{\gamma-1}{\alpha_T}\rho C_V\nabla\cdot\boldsymbol{u} - \boldsymbol{\Pi}:\nabla\boldsymbol{u} + \eta\frac{|\nabla\times\boldsymbol{B}|^2}{\mu_0} - \nabla\cdot\boldsymbol{q}. \tag{20}$$

Finally in the section, we write the governing equations (15a), (15b), (15c), and (20) in terms of only density, bulk flow velocity, magnetic field, temperature, and constitutive parameters of the fluid—in other words, we substitute for the pressure p the viscosity tensor $\boldsymbol{\Pi}$ and the heat flux $\boldsymbol{q}$ in terms of the aforementioned variables. To eliminate the pressure, we use thermodynamic identity

$$\nabla p = \frac{c_s^2}{\gamma}(\nabla\rho + \rho\alpha_T\nabla T), \tag{21}$$

for c_s the adiabatic sound speed (see Appendix A). For the viscosity tensor and heat flux, we use constitutive relations

$$\boldsymbol{\Pi} = -\zeta_s\left[\nabla\boldsymbol{u} + (\nabla\boldsymbol{u})^T - \frac{2}{3}(\nabla\cdot\boldsymbol{u})\mathbf{I}\right] - \zeta_b(\nabla\cdot\boldsymbol{u})\mathbf{I}, \tag{22a}$$

$$\boldsymbol{q} = -\kappa\nabla T, \tag{22b}$$

where ζ_s is the first coefficient of viscosity (or shear viscosity), ζ_b the second coefficient of viscosity (or bulk viscosity), $\mathbf{I}$ the identity tensor, and κ the thermal conductivity. We note that for sufficiently large magnetic fields, the chosen constitutive relations may not be appropriate; for example, it is well known that $\boldsymbol{q}$ is predominantly parallel to $\boldsymbol{B}$ in weakly coupled collisional plasma where the Larmor radius r_{ce} of constituent thermal electrons satisfies $r_{ce} \ll \lambda_{ei}$ [11]. However, the calculation presented here is easily modified to include such effects if necessary. Furthermore, provided the thermal and magnetic energy densities in the plasma are comparable (that is, $\beta \equiv 2\mu_0 p/B^2 \sim 1$), it follows that $r_{ce} \sim \beta^{1/2}d_e \gg \lambda_{ei}$, suggesting that magnetic fields do not affect plasma transport properties in this case.

On substituting (22), we find our desired system of equations:

$$\frac{d\rho}{dt} = -\rho\nabla\cdot\boldsymbol{u}, \tag{23a}$$

$$\rho\frac{d\boldsymbol{u}}{dt} = -\frac{c_s^2}{\gamma}(\nabla\rho + \rho\alpha_T\nabla T) + \frac{(\nabla\times\boldsymbol{B})\times\boldsymbol{B}}{\mu_0} + \nabla(\zeta_b\nabla\cdot\boldsymbol{u}) + \nabla\cdot\left\{\zeta_s\left[\nabla\boldsymbol{u} + (\nabla\boldsymbol{u})^T - \frac{2}{3}(\nabla\cdot\boldsymbol{u})\mathbf{I}\right]\right\}, \tag{23b}$$

$$\frac{d\boldsymbol{B}}{dt} = \boldsymbol{B}\cdot\nabla\boldsymbol{u} - \boldsymbol{B}\nabla\cdot\boldsymbol{u} - \nabla\times(\eta\nabla\times\boldsymbol{B}), \tag{23c}$$

$$\rho\frac{dT}{dt} = -\frac{\gamma-1}{\alpha_T}\rho\nabla\cdot\boldsymbol{u} - \frac{1}{C_V}\boldsymbol{\Pi}:\nabla\boldsymbol{u} + \eta\frac{|\nabla\times\boldsymbol{B}|^2}{\mu_0 C_V} + \frac{1}{C_V}\nabla\cdot(\kappa\nabla T), \tag{23d}$$

where for brevity we have not written out in full the viscous dissipation term in the temperature evolution equation. Note that these equations do not necessarily assume that the matter's transport coefficients (specifically ζ_s, ζ_b, η, and κ) are independent of temperature or density.

IV. FLUCTUATIONS AND THE DYNAMIC STRUCTURE FACTOR

We now evaluate the MHD dynamic structure factor in the limit of small-amplitude fluctuations. To perform this calculation, we consider some equilibrium state, with density ρ_0, no bulk flow motion, magnetic field $\boldsymbol{B}_0$, temperature T_0, sound speed c_{s0}, adiabatic index γ_0, coefficient of thermal expansion α_{T0}, bulk viscosity ζ_{b0}, shear viscosity ζ_{s0}, resistivity η_0, specific heat capacity at constant volume C_{V0}, and thermal conductivity κ_0. We then consider small-amplitude fluctuations of dynamic quantities on this equilibrium:

$$\rho = \rho_0 + \delta\rho, \quad \boldsymbol{u} = \delta\boldsymbol{u}, \quad \boldsymbol{B} = \boldsymbol{B}_0 + \delta\boldsymbol{B}, \quad T = T_0 + \delta T. \tag{24}$$

The small-fluctuation assumption of dynamic quantities is natural for a fluid system in (or close to) equilibrium, because the typical relative magnitude $\delta\rho/\rho_0$ of thermal density fluctuations on the fluid scale L compared to the mean density satisfies $\delta\rho/\rho_0 \sim n^{-2/3}L^{-2} \ll 1$ (where the last inequality must hold for any fluid system). Nevertheless, this statement necessitates two implicit assumptions. First, the results of our subsequent calculation do not apply if the system is in fact far from equilibrium. This includes matter supporting a shock wave or turbulent fluids. Second, both the total photon intensity I_0 and pulse energy must be sufficiently low as to not perturb the fluid system significantly. It is well known that resonant plasma instabilities triggered by electromagnetic radiation of sufficiently high-intensity can be avoided if $(I_0/10^{15}\ \mathrm{W\,cm^{-2}})(\lambda_0/1\ \mu\mathrm{m})^2 \lesssim 1$ (for λ_0 the incident wavelength) [24], while heating due to inverse Bremstrahllung is insignificant provided the associated change in electron temperature ΔT_e—which can be estimated as

$$\Delta T_e \approx 0.5\left(\frac{Z}{5.7}\right)\left(\frac{n_e}{10^{23}\ \mathrm{cm^{-3}}}\right)\left(\frac{T_e}{50\ \mathrm{eV}}\right)^{-3/2}\left(\frac{\lambda_0}{5\ \mathrm{nm}}\right)^3 \times\left\{1-\exp\left[-\frac{(\hbar\omega_0/250\ \mathrm{eV})}{(k_B T_e/50\ \mathrm{eV})}\right]\right\} \times\left(\frac{I_0}{10^{15}\ \mathrm{W\,cm^{-2}}}\right)\left(\frac{\Delta\tau}{100\ \mathrm{fs}}\right)\mathrm{eV}, \tag{25}$$

for $\Delta\tau$ the total pulse duration [7]—satisfies $\Delta T_e \ll T_e$.

Substituting linearization (24) into (23a), (23b), (23c), and (23d), and neglecting terms quadratic or higher in fluctuating quantities, we find

$$\frac{\partial\delta\rho}{\partial t} = -\rho_0\nabla\cdot\delta\boldsymbol{u}, \tag{26a}$$

$$\rho_0\frac{\partial\delta\boldsymbol{u}}{\partial t} = -\frac{c_{s0}^2}{\gamma_0}(\nabla\delta\rho + \rho_0\alpha_{T0}\nabla\delta T) + \frac{\boldsymbol{B}_0\cdot\nabla\delta\boldsymbol{B}}{\mu_0} - \nabla\left(\frac{\boldsymbol{B}_0\cdot\delta\boldsymbol{B}}{\mu_0}\right) + \zeta_{s0}\nabla^2\delta\boldsymbol{u} + \zeta_{c0}\nabla(\nabla\cdot\delta\boldsymbol{u}), \tag{26b}$$

$$\frac{\partial\delta\boldsymbol{B}}{\partial t} = \boldsymbol{B}_0\cdot\nabla\delta\boldsymbol{u} - \boldsymbol{B}_0\nabla\cdot\delta\boldsymbol{u} + \eta_0\nabla^2\delta\boldsymbol{B}, \tag{26c}$$

$$\frac{\partial\delta T}{\partial t} = -\frac{\gamma_0-1}{\alpha_{T0}}\nabla\cdot\delta\boldsymbol{u} + \gamma_0\chi_0\nabla^2\delta T, \tag{26d}$$

where we have defined "compressive" viscosity coefficient $\zeta_{c0} \equiv \zeta_{b0} - 2\zeta_{s0}/3$ and thermal diffusivity $\chi_0 \equiv \kappa_0/\rho_0 C_{V0}\gamma_0$.

To find the dynamic structure factor, we transform Eqs. (26) using a Fourier transform in space and a Laplace transform in time. For vector quantity $\delta\boldsymbol{x}$, this operation is defined as

$$\widetilde{\delta\boldsymbol{x}}_{\boldsymbol{k}}(s) = \int_0^\infty dt\, e^{-st}\int d^3\boldsymbol{r}\, e^{i\boldsymbol{k}\cdot\boldsymbol{r}}\,\delta\boldsymbol{x}(\boldsymbol{r},t).$$

Applying this, and using standard properties of Laplace and Fourier transforms under derivatives, we find

$$s\widetilde{\delta\rho}_{\boldsymbol{k}}(s) = -\rho_0 i\boldsymbol{k}\cdot\widetilde{\delta\boldsymbol{u}}_{\boldsymbol{k}}(s) + \delta\rho_{\boldsymbol{k}}(0), \tag{27a}$$

$$\rho_0 s\widetilde{\delta\boldsymbol{u}}_{\boldsymbol{k}}(s) = -\frac{c_{s0}^2}{\gamma_0}[i\boldsymbol{k}\widetilde{\delta\rho}_{\boldsymbol{k}}(s) + i\rho_0\alpha_{T0}\boldsymbol{k}\widetilde{\delta T}_{\boldsymbol{k}}(s)] + i\widetilde{\delta\boldsymbol{B}}_{\boldsymbol{k}}(s)\frac{\boldsymbol{B}_0\cdot\boldsymbol{k}}{\mu_0} - i\boldsymbol{k}\frac{\boldsymbol{B}_0\cdot\widetilde{\delta\boldsymbol{B}}_{\boldsymbol{k}}(s)}{\mu_0} - \zeta_{s0}k^2\widetilde{\delta\boldsymbol{u}}_{\boldsymbol{k}}(s) - \zeta_{c0}\boldsymbol{k}[\boldsymbol{k}\cdot\widetilde{\delta\boldsymbol{u}}_{\boldsymbol{k}}(s)] + \rho_0\delta\boldsymbol{u}_{\boldsymbol{k}}(0), \tag{27b}$$

$$s\widetilde{\delta\boldsymbol{B}}_{\boldsymbol{k}}(s) = i(\boldsymbol{k}\cdot\boldsymbol{B}_0)\widetilde{\delta\boldsymbol{u}}_{\boldsymbol{k}}(s) - i\boldsymbol{B}_0[\boldsymbol{k}\cdot\widetilde{\delta\boldsymbol{u}}_{\boldsymbol{k}}(s)] - \eta_0 k^2\widetilde{\delta\boldsymbol{B}}_{\boldsymbol{k}}(s) + \delta\boldsymbol{B}_{\boldsymbol{k}}(0), \tag{27c}$$

$$s\widetilde{\delta T}_{\boldsymbol{k}}(s) = -i\frac{\gamma_0-1}{\alpha_{T0}}\boldsymbol{k}\cdot\widetilde{\delta\boldsymbol{u}}_{\boldsymbol{k}}(s) - \gamma_0\chi_0 k^2\widetilde{\delta T}_{\boldsymbol{k}}(s) + \delta T_{\boldsymbol{k}}(0). \tag{27d}$$

The dynamic structure factor $S_{nn}(\boldsymbol{k},\omega)$ is related to the transformed fluctuating quantities via the following limit of the density autocorrelation function [18]:

$$\frac{S_{nn}(\boldsymbol{k},\omega)}{S_{nn}(\boldsymbol{k})} = 2\mathrm{Re}\left[\lim_{\varepsilon\to 0}\frac{\langle\delta\rho_{\boldsymbol{k}}^*(0)\widetilde{\delta\rho}_{\boldsymbol{k}}(s=\varepsilon+i\omega)\rangle}{\langle\delta\rho_{\boldsymbol{k}}^*(0)\delta\rho_{\boldsymbol{k}}(0)\rangle}\right], \tag{28}$$

where we have used the definition

$$S_{nn}(\boldsymbol{k}) = \int d\omega\, S_{nn}(\boldsymbol{k},\omega)d\omega, \tag{29}$$

which is usually referred to as the static structure factor.

To find an explicit expression for $S(\boldsymbol{k},\omega)$, we solve Eqs. (27) for $\widetilde{\delta\rho_{\boldsymbol{k}}}(s)$ before evaluating the density autocorrelation function. We find that

$$\frac{\langle\delta\rho^*_{\boldsymbol{k}}(0)\widetilde{\delta\rho_{\boldsymbol{k}}}(s)\rangle}{\langle\delta\rho^*_{\boldsymbol{k}}(0)\delta\rho_{\boldsymbol{k}}(0)\rangle}=\frac{P(k,s)}{Q(k,s)}, \tag{30}$$

where

$$\begin{aligned}P(k,s)&=(s+\gamma_0\chi_0k^2)(s+\nu_{l0}k^2)(s+\eta_0k^2)(s+\nu_{s0}k^2)\\&\quad+\frac{\gamma_0-1}{\gamma_0}k^2c_{s0}^2(s+\eta_0k^2)(s+\nu_{s0}k^2)\\&\quad+k^2v_A^2(s+\gamma_0\chi_0k^2)(s+k^2[\nu_{s0}+\nu_{c0}\cos^2\theta])\\&\quad+\frac{\gamma_0-1}{\gamma_0}k^4v_A^2c_0^2\cos^2\theta,\end{aligned} \tag{31a}$$

$$\begin{aligned}Q(k,s)&=\frac{k^2c_{s0}^2}{\gamma_0}(s+\gamma_0\chi_0k^2)(s+\eta_0k^2)(s+\nu_{s0}k^2)\\&\quad+\frac{1}{\gamma_0}k^4v_A^2c_0^2\cos^2\theta(s+\gamma_0\chi_0k^2)\\&\quad+sP(k,s).\end{aligned} \tag{31b}$$

Here we define various additional quantities: shear kinematic viscosity $\nu_{s0}\equiv\zeta_{s0}/\rho_0$, compressive kinematic viscosity $\nu_{c0}=\zeta_{c0}/\rho_0$, longitudinal viscosity $\nu_{l0}=\nu_{s0}+\nu_{c0}$, θ the angle between $\boldsymbol{B}_0$ and $\boldsymbol{k}$, and v_A the Alfvèn speed:

$$v_A\equiv\frac{B_0}{\sqrt{\mu_0\rho_0}}, \tag{32}$$

(where $B_0=|\boldsymbol{B}_0|$). Full details of this calculation are presented in Appendix B; we note for clarity's sake that the derivation of (30) assumes that the initial density fluctuations are uncorrelated with the initial velocity, magnetic field, and temperature fluctuations.

In principle, one can now calculate the dynamic structure factor using (28) to give this paper's main result. However, performing the general calculation analytically is tedious; it is more physically elucidating to instead consider various special cases of the dynamic structure factor first, where analytical calculations can be undertaken more readily. These are presented next.

V. PARALLEL FLUCTUATIONS

We first consider fluctuations whose wave vector is parallel to the magnetic field: in other words, $\cos\theta=1$. In this case, it is elementary to show that

$$P(k,s)=\left[(s+\eta_0k^2)(s+\nu_{s0}k^2)+k^2v_A^2\right]P_\parallel(k,s), \tag{33a}$$

$$Q(k,s)=\left[(s+\eta_0k^2)(s+\nu_{s0}k^2)+k^2v_A^2\right]Q_\parallel(k,s), \tag{33b}$$

where

$$P_\parallel(k,s)=(s+\gamma_0\chi_0k^2)(s+\nu_{l0}k^2)+\frac{\gamma_0-1}{\gamma_0}k^2c_{s0}^2, \tag{34a}$$

$$Q_\parallel(k,s)=\frac{k^2c_{s0}^2}{\gamma_0}(s+\gamma_0\chi_0k^2)+sP_\parallel(k,s). \tag{34b}$$

The density autocorrelation function becomes

$$\frac{\langle\delta\rho^*_{\boldsymbol{k}}(0)\widetilde{\delta\rho_{\boldsymbol{k}}}(s)\rangle}{\langle\delta\rho^*_{\boldsymbol{k}}(0)\delta\rho_{\boldsymbol{k}}(0)\rangle}=\frac{P_\parallel(k,s)}{Q_\parallel(k,s)}. \tag{35}$$

We then consider the limit where the dissipation rate of fluctuations is much smaller than the frequency, that is,

$$|s|\sim\omega\gg\chi_0k^2,\eta_0k^2,\nu_{s0}k^2,\nu_{l0}k^2. \tag{36}$$

Expanding (35) in this limit (see Appendix C for an outline of the expansion technique), and then calculating $S_{nn}(k,\omega)$ using (28), we find

$$\begin{aligned}\frac{S_{nn}(k,\omega)}{S_{nn}(k)}&\approx\frac{\gamma_0-1}{\gamma_0}\frac{2\chi_0k^2}{\omega^2+(\chi_0k^2)^2}\\&\quad+\frac{1}{\gamma_0}\left[\frac{\Gamma_\parallel k^2}{(\Gamma_\parallel k^2)^2+(\omega+c_{s0}k)^2}\right.\\&\quad\left.+\frac{\Gamma_\parallel k^2}{(\Gamma_\parallel k^2)^2+(\omega-c_{s0}k)^2}\right],\end{aligned} \tag{37}$$

where

$$\Gamma_\parallel=\frac{(\gamma_0-1)\chi_0+\nu_{l0}}{2}. \tag{38}$$

The resulting structure factor is identical to the hydrodynamic structure factor [21]: there are three peaks, two of which are associated with sound waves (so-called Brillouin peaks) and one is associated with the entropy mode (the elastic peak). The location of the Brillouin peaks is given by the dispersion relation of sound waves; the dependence of their width on both viscosity and thermal diffusivity via $\Gamma_\parallel$ is reflective of the fact that both viscous and conductive losses damp sound waves. The elastic peak has zero frequency on account of the nonpropagating nature of the entropy mode; the thermal diffusivity alone determines the width, because for small-amplitude fluctuations, conductive losses consititute the primary damping mechanism for the mode. The reason that the MHD structure factor for parallel wave numbers is identical to the hydrodynamic one is simply that parallel compressive fluctuations in MHD do not interact the magnetic field. Parallel fluctuations of the magnetic field can exist (in particular, Alfvèn waves) but do not have a density perturbation associated with them.

VI. QUASIPERPENDICULAR FLUCTUATIONS

Next, we turn to perturbations which are almost perpendicular to the magnetic field; in other words, $\cos\theta\ll1$. We also assume that the thermal and magnetic energy densities of the equilibrium are comparable; mathematically, this is equivalent to ordering $v_A\sim c_{s0}$. This regime is relevant for intergalactic plasma, where tiny magnetic fields are amplified and brought to equipartition via the turbulent dynamo mechanism [25]. This also applies to laboratory turbulent plasmas when the resistivity is small enough that magnetic field dissipation becomes very weak [26].

In this case, again considering the approximation (36) it can be shown that (see Appendix C)

$$\frac{S_{nn}(k,\omega)}{S_{nn}(k)} \approx \frac{\gamma_0-1}{\gamma_0}\frac{2\chi_0 k^2}{\omega^2+(\chi_0 k^2)^2} + \frac{1}{\gamma_0}\frac{v_A^2}{c_{FW}^2}\left[\frac{\Gamma_{SW}k^2}{(\Gamma_{SW}k^2)^2+(\omega+c_{SW}k)^2}+\frac{\Gamma_{SW}k^2}{(\Gamma_{SW}k^2)^2+(\omega-c_{SW}k)^2}\right] + \frac{1}{\gamma_0}\frac{c_{s0}^2}{c_{FW}^2}\left[\frac{\Gamma_{FW}k^2}{(\Gamma_{FW}k^2)^2+(\omega+c_{FW}k)^2}+\frac{\Gamma_{FW}k^2}{(\Gamma_{FW}k^2)^2+(\omega-c_{FW}k)^2}\right], \tag{39}$$

where

$$c_{SW} = \frac{v_A\cos\theta}{\sqrt{1+v_A^2/c_{s0}^2}}, \tag{40a}$$

$$c_{FW} = \sqrt{c_{s0}^2+v_A^2}, \tag{40b}$$

and

$$\Gamma_{SW} = \frac{1}{2}\left[(\gamma_0-1)\frac{v_A^2}{c_{FW}^2}\chi_0 + \frac{c_{s0}^2}{c_{FW}^2}\eta_0 + \nu_{s0}\right], \tag{41a}$$

$$\Gamma_{FW} = \frac{1}{2}\left[(\gamma_0-1)\frac{c_{s0}^2}{c_{FW}^2}\chi_0 + \frac{v_A^2}{c_{FW}^2}\eta_0 + \nu_{l0}\right]. \tag{41b}$$

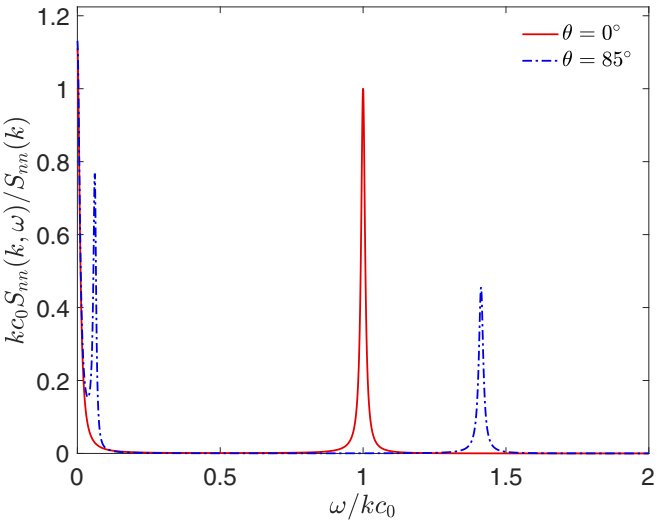

FIG. 3. The dynamic structure factor in magnetized, high-density plasma for parallel and quasiperpendicular scattering vectors. At a given angle θ between the scattering vector and the magnetic field, the dynamic structure factor is calculated by first evaluating the density autocorrelation function using (30) before taking the limit specified in (28). The structure factor is presented in a dimensionless form; this is obtained via $s \mapsto skc_{s0}$. For an aluminum plasma with $n_e = 10^{23}$ cm^{-3} and $T = 50$ eV ($Z \approx 5.7$), any photon with initial frequency ω_0 in the range 4.7×10^{16} s$^{-1} \ll \omega_0 \ll 5.3\times10^{17}$ s^{-1} is in the relevant regime (see Sec. II); the corresponding shift in frequency $\omega = kc_{s0}$ associated with the Brillouin peaks then satisfies 6.6×10^{12} s$^{-1} \ll \omega \ll 7.7\times10^{13}$ s^{-1} (where we have calculated sound speed $c_{s0} = \sqrt{\gamma Zk_BT/Mm_p} \approx 40$ km s^{-1}). With this mapping, the magnitude of the various dissipative terms are represented by the dimensionless numbers $k\chi_0/c_{s0}$, $k\eta_0/c_{s0}$, $k\nu_{s0}/c_{s0}$, and $k\nu_{c0}/c_{s0}$. Parallel ($\theta = 0°$) and quasiperpendicular ($\theta = 85°$) are plotted. The peak magnitude in each example is normalized to the parallel case. For this particular plot, we choose $v_A = c_{s0}$, $k\chi_0/c_{s0} = 0.01$, $k\eta_0/c_{s0} = 0.01$, $k\nu_{s0}/c_{s0} = 0.0067$, and $k\nu_{c0}/c_{s0} = 0.0033$.

By comparison to the pure hydrodynamic case (37), we immediately note a number of similarities and differences. Most significantly, the dynamic structure factor for quasiperpendicular modes has five peaks rather than three. The elastic peak remains unchanged, and there still exist two peaks at frequencies $\omega \gtrsim kc_{s0}$. However, the frequency position of these peaks is now also dependent on the magnetic field and is greater than the sound speed: $\omega = kc_{FW} > kc_{s0}$. In addition, a new pair of peaks has emerged with characteristic frequency much smaller than the sound speed ($\omega = kc_{SW} \sim kv_A\cos\theta \ll kc_{s0}$). The width and heights of both peaks are comparable and depend on the viscosity, resistivity, and thermal diffusivity.

The emergence of the additional peaks and their subsequent characteristics can again be explained physically. More specifically, in MHD one finds two distinct quasiperpendicular modes with density perturbations: the fast and slow magnetosonic waves. Fast magnetosonic waves are conceptually similar to sound waves, except for the effective equilibrium pressure being increased by additional magnetic pressure: in fast waves, the magnetic and thermal pressure fluctuations are in phase. By constrast, slow magnetosonic waves are almost incompressible ($\boldsymbol{\nabla}\cdot\delta\boldsymbol{u} \sim \cos\theta \ll 1$), with magnetic and thermal pressure fluctuations acting out of phase. Both magnetosonic waves in general have significant magnetic and thermal components and thus are both subject to resistive and conductive damping; however, the effective viscosity experienced by the waves is different, on account of the quasi-incompressibility of slow magnetosonic waves. Finally, the entropy mode is unchanged in MHD and does not have a magnetic component; thus, it is not surprising that the elastic peak is unchanged.

We illustrate these claims numerically in Fig. 3, which shows the dynamic structure factor evaluated for parallel and quasiperpendicular modes using Eqs. (28) and (30) for $v_A = c_{s0}$ and weak dissipation terms (see caption for details). As anticipated, for parallel modes the MHD dynamic structure factor is identical to the hydrodynamic one. However, for quasiperpendicular modes, we observe two scattering peaks at positive frequencies, whose positions are strongly separated.

VII. OBLIQUE FLUCTUATIONS

Finally returning to the case of oblique fluctuations, we can now anticipate that the dynamic structure factor will have five peaks: an entropy peak and four additional peaks. The approximate positions of these peaks can be obtained by considering roots of $Q(k,s)$ when all diffusive effects are completely neglected:

$$Q(k,s) \approx s\left[s^4 + \left(k^2c_{s0}^2 + k^2v_A^2\right)s^2 + k^4v_A^2c_{s0}^2\cos^2\theta\right]. \tag{42}$$

The five roots are then

$$s^2 = 0, -\tfrac{1}{2}k^2\left[c_{s0}^2 + v_A^2 \pm \sqrt{\left(c_{s0}^2 + v_A^2\right)^2 - 4c_{s0}^2 v_A^2 \cos^2\theta}\right], \tag{43}$$

with associated peak frequencies

$$\omega^2 = 0, \tfrac{1}{2}k^2\left[c_{s0}^2 + v_A^2 \pm \sqrt{\left(c_{s0}^2 + v_A^2\right)^2 - 4c_{s0}^2 v_A^2 \cos^2\theta}\right]. \tag{44}$$

The "+" roots correspond to the fast magnetosonic modes and the "−" roots to the slow magnetosonic modes. We note that for $c_{s0} \sim v_A$, and $\cos\theta \lesssim 1$, the fast and slow magnetosonic modes have frequencies with a comparable order of magnitude at a given wave number but that the fast magnetosonic mode's frequency is always greater. For quasiparallel modes, the frequencies are very similar; for quasiperpendicular, they have different orders of magnitude. The width and height of the peaks are controlled by (in general, quite complicated) linear combinations of the resistivity, thermal diffusivity, and the viscosities. These claims are demonstrated in Fig. 4, where the dynamic structure factor is again calculated numerically using Eqs. (28) and (30). For oblique modes, we observe two scattering peaks at positive frequencies comparable to the sound speed, whose positions become increasingly separated as θ is increased.

One further special case which can be treated analytically is that of a weak but finite magnetic field: $v_A \ll c_{s0}$, but $v_A/k\chi_0, v_A/k\eta_0, v_A/k\nu_{l0} \gg 1$. As well as being tractable, this regime is conceptually interesting because it is relevant to understanding the transition between unmagnetized and magnetized matter. In this regime, the frequency ω_{FW} of the fast magnetosonic mode greatly exceeds the slow mode ω_{SW}:

$$\omega_{FW} \approx kc_{s0} \gg \omega_{SW} \approx kv_A\cos\theta. \tag{45}$$

This separation of frequencies again allows for an analytical form of the dynamic structure factor to be derived:

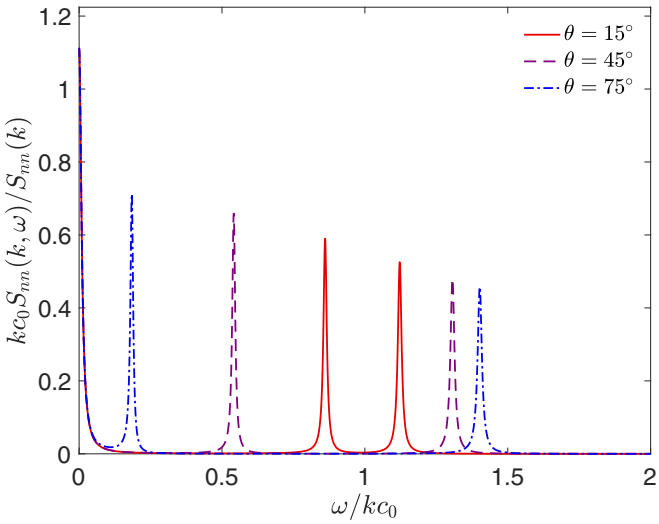

FIG. 4. The dynamic structure factor in magnetized, high-density plasma at oblique scattering angles. The plotted dynamic structure factors are calculated at a given angle in the same way as Fig. 3, with the same dimensionless values for the dissipative terms. Three angles are plotted in Fig. 1: $\theta = 15°, \theta = 45°$, and $\theta = 75°$. The peak magnitude in each example is again normalized to the parallel case.

$$\frac{S_{nn}(k,\omega)}{S_{nn}(k)} \approx \frac{\gamma_0 - 1}{\gamma_0}\frac{2\chi_0 k^2}{\omega^2 + \left(\chi_0 k^2\right)^2} + \frac{1}{\gamma_0}\frac{v_A^2}{c_{s0}^2}\left[\frac{\Gamma_A k^2}{(\Gamma_A k^2)^2 + (\omega + c_A k)^2} + \frac{\Gamma_A k^2}{(\Gamma_A k^2)^2 + (\omega - c_A k)^2}\right] + \frac{1}{\gamma_0}\left[\frac{\Gamma_\parallel k^2}{(\Gamma_\parallel k^2)^2 + (\omega + c_{s0} k)^2} + \frac{\Gamma_\parallel k^2}{(\Gamma_\parallel k^2)^2 + (\omega - c_{s0} k)^2}\right], \tag{46}$$

where

$$c_A \equiv v_A\cos\theta, \tag{47a}$$

$$\Gamma_A = \frac{\eta_0 + \nu_{s0}}{2}. \tag{47b}$$

In this regime, we see that both the Brillouin peaks and the entropy peak remain unaltered from their hydrodynamic form; however, an additional peak exists, whose peak amplitude is proportional to v_A^2/c_{s0}^2. Thus, as the magnetization increases, it is anticipated that an additional pair of peaks would emerge in the dynamic structure factor, with their amplitude solely a function of the magnetic field strength. In addition, we note that the width of these additional peaks is a function of the resistivity and kinematic shear viscosity alone. This is because slow magnetosonic waves in the limit $v_A \ll c_{s0}$ have asymptotically small temperature and compressive velocity perturbations, and so dissipation via the bulk viscosity or thermal diffusivity is very weak. These claims are demonstrated numerically in Fig. 5, where for a fixed angle increasing values of v_A/c_{s0} are presented.

VIII. DETAILED BALANCE

So far we have discussed the scattering cross section as essentially a classical process. We expect this to be a good approximation since we have been considering the collective Thomson scattering response associated with low-frequency excitations whose characteristic phase velocities are comparable to ion rather than electron motions [27]. Some quantum effects are implicitly accounted for from the specific form of the transport coefficients; others, such as diffraction and nonlocality, are not. The relevant restriction on the scattering wave number k associated with the latter effects is $k\lambda_{th} \ll 1$, where $\lambda_{th} = 9.8 \times 10^{-9}(T/50\ \mathrm{eV})^{-1/2}$ cm is the thermal de Broglie wavelength [28]. Similarly to (8), this can be written

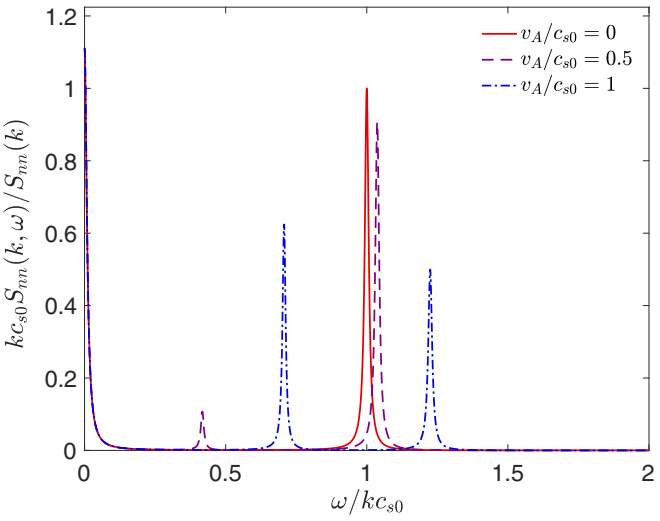

FIG. 5. The dynamic structure factor in magnetized, high-density plasma with increasing magnetization. The plotted dynamic structure factors are calculated in the same way as in Fig. 3, with the same dimensionless values for the dissipative terms. However, in contrast to Fig. 3, the angle of fluctuations with respect to the magnetic field θ is fixed at $\theta = 30^\circ$, while the strength of the magnetic field is increased from nothing ($v_A/c_{s0} = 0$) via a subdominant magnetic field ($v_A/c_{s0} = 0.5$) to a field in equipartition ($v_A/c_{s0} = 1$).

as an upper bound on photon energy:

$$\hbar\omega_0 \ll 2.0 \times 10^3 \left(\frac{T}{50\ \text{eV}}\right)^{1/2} \text{eV}. \tag{48}$$

The requirement that this condition on the photon energy and propagation condition (9) be satisfied places another constraint on the plasma density at a given temperature: $\lambda_{th} \ll d_e$, or

$$n_e \ll 2.9 \times 10^{27} \left[\frac{\sec(\theta_T/60^\circ)}{2}\right]^{-2} \left(\frac{T}{50\ \text{eV}}\right)^{-1}. \tag{49}$$

This constraint is depicted in Fig. 1. We note that our calculation does in fact apply to some degenerate plasmas, in which

$$\Theta \equiv \frac{h n_e^{1/3}}{\sqrt{3 m_e k_B T}} \sim \frac{\lambda_{th}}{n_e^{-1/3}} \gtrsim 1. \tag{50}$$

This is because the constraint $kn^{-1/3} \ll 1$ can be rewritten as $k\lambda_{th} \ll \Theta^{-1}$, which in turn guarantees (48) for $\Theta \sim 1$. Nevertheless, the neglect of these quantum effects provide the strongest upper bound on the characteristic electron number densities to which our calculation applies. This all being said, higher-order quantum corrections can in principle be included in the MHD formalism discussed here via the introduction of the Bohm potential [22,29].

In addition to this, quantum effects directly associated with detailed balance are not always negligible, especially if we are dealing with low-frequency excitations, as in the present work. These effects, however, can be brought back in the cross section via the prescription [27,30]

$$S_{nn}(\boldsymbol{k}, \omega) \to \frac{\hbar\omega/k_B T}{1 - e^{-\hbar\omega/k_B T}} S_{nn}(\boldsymbol{k}, \omega). \tag{51}$$

IX. CONCLUDING REMARKS

In this paper we have discussed the structure of the Thomson scattering cross section in a nonrelativistic, dense, magnetized plasma, where collective excitations are most appropriately described via magnetohydrodynamics. We have found that, in addition to cyclotron resonances, the form of the structure factor is dependent on the angle of fluctuations with respect to the large-scale magnetic field present in the matter. For parallel fluctuations, the dynamic structure factor is the same as the hydrodynamic one. However, for oblique fluctuations an additional pair of peaks emerges, which are associated with fluctuations of the magnetic field in combination with density fluctuations. For quasiperpendicular fluctuations, there exists a large discrepancy between the frequency of the two peaks of the order of the parallel wave number divided by the total wave number. The existence of the additional pair of peaks holds irrespective of the exact nature of momentum and heat transport in the plasma, provided the general diffusion rates associated with the transport are small compared to the frequencies of fluctuations.

We observe that the qualitative features of the calculated Thomson scattering cross section also apply to all collisional magnetized plasmas, weakly or strongly coupled, provided frequencies ω and wave numbers k are sufficiently small when compared to electron collision rates and mean free paths. This is because magnetohydrodynamics is an appropriate model for collisional plasma on large scales, irrespective of the coupling parameter—for example, exact constitutive relations for weakly coupled plasma can be derived formally using kinetic theory [11]. We note that the Thomson scattering cross section has been evaluated previously for weakly coupled plasma using kinetic theory, including a collision operator [10]. However, such calculations usually assume that the equilibrium distribution of the plasma is Maxwellian, with spatially constant macroscopic parameters (density, temperature, and magnetic field). By contrast, large-scale magnetohydrodynamic modes require spatially varying macroscopic parameters, and so the associated peaks do not seem to be captured in this previous work. That being said, it should be emphasized that the kinetic theory calculations describe collective excitations in a weakly coupled plasma on small wave number scales $k\lambda_{ei} \gtrsim 1$ which are not present in the magnetohydrodynamical model.

From an experimental point of view, we note that the existence of many peaks in the scattering spectra allow for the simultaneous measurement of the sound speed and the magnetic field in magnetized dense plasma. From our calculations, we anticipate that the necessary magnetic field strength for a noticeable effect corresponds to approximately equal Alfvén and sound speeds; assuming an ideal gas law for the pressure, this can be written as

$$B \approx 12 \left(\frac{\gamma}{5/3}\right) \left(\frac{n_e}{10^{23}\ \text{cm}^{-3}}\right)^{1/2} \left(\frac{T}{50\ \text{eV}}\right)^{1/2} \text{MG}. \tag{52}$$

Thus, we anticipate that our calculations could be of relevance to a range of magnetized laboratory plasmas, including high-density laser plasmas generated by short-pulse lasers [31] or Z-pinch plasma [32]. In addition to this, the width of both peaks can be used to constrain transport properties in

such plasma, although the resistivity, bulk viscosity, and shear viscosity cannot be measured simultaneously (unless one or more of these transport coefficients is known to be small). This implies that Thomson scattering can be implemented as a powerful diagnostics tool for plasma properties that are otherwise very challenging to measure [7].

ACKNOWLEDGMENTS

The research leading to these results has received funding from AWE plc. and the Engineering and Physical Sciences Research Council (Grants No. EP/M022331/1 and No. EP/N014472/1) of the United Kingdom.

APPENDIX A: THERMODYNAMIC IDENTITIES

In this Appendix, we derive Eqs. (19) and (21) for the specific entropy and pressure in terms of state variables temperature and density and constitutive parameters of the matter. Assuming that specific entropy $\mathcal{S} = \mathcal{S}(\rho, T)$, the total differential is given by

$$d\mathcal{S} = \left(\frac{\partial \mathcal{S}}{\partial \rho}\right)_T d\rho + \left(\frac{\partial \mathcal{S}}{\partial T}\right)_\rho dT. \tag{A1}$$

Using the reciprocal identity, reciprocity, and Maxwell's identities, it follows that

$$\left(\frac{\partial \mathcal{S}}{\partial \rho}\right)_T = -\frac{1}{\rho^2}\left(\frac{\partial p}{\partial T}\right)_\rho = \frac{C_V - C_P}{\alpha_T \rho T}, \quad \left(\frac{\partial \mathcal{S}}{\partial T}\right)_\rho = \frac{C_V}{T}, \tag{A2}$$

where C_P is the heat capacity at constant pressure, and the coefficient of thermal expansion is defined by $\alpha_T = -\rho^{-1}(\partial\rho/\partial T)_p$. We conclude that

$$dS = \frac{C_V}{T}\left(dT - \frac{\gamma - 1}{\alpha_T} d\rho\right), \tag{A3}$$

where we have used $\gamma = C_P/C_V$. This translates immediately into (19).

Similarly, the pressure $p = p(\rho, T)$ leads to total differential

$$dp = \left(\frac{\partial p}{\partial \rho}\right)_T d\rho + \left(\frac{\partial p}{\partial T}\right)_\rho dT. \tag{A4}$$

Reciprocity and Maxwell's identities then give

$$\left(\frac{\partial p}{\partial \rho}\right)_T = \frac{C_V}{C_P}\left(\frac{\partial p}{\partial \rho}\right)_\mathcal{S} = \frac{c_s^2}{\gamma}, \quad \left(\frac{\partial p}{\partial T}\right)_\rho = \left(\frac{\partial p}{\partial \rho}\right)_T \left(\frac{\partial \rho}{\partial T}\right)_p = \frac{c_s^2}{\gamma}\alpha_T \rho, \tag{A5}$$

using the definition $c_s^2 \equiv (\partial p/\partial \rho)_\mathcal{S}$ for the adiabatic sound speed. This implies that

$$dp = \frac{c_s^2}{\gamma}(d\rho + \rho\alpha_T\, dT), \tag{A6}$$

from which (21) follows trivially.

APPENDIX B: SOLVING FOR THE DENSITY AUTOCORRELATION FUNCTION

Here we describe the method used to derive Eq. (30) from Eqs. (27). We begin by assuming that the initial density fluctuations $\delta\rho_{\boldsymbol{k}}(0)$ are uncorrelated with the initial temperature fluctuations $\delta T_{\boldsymbol{k}}(0)$, the initial velocity fluctuations $\delta \boldsymbol{u}_{\boldsymbol{k}}(0)$, and the initial magnetic field fluctuations $\delta \boldsymbol{B}_{\boldsymbol{k}}(0)$. This assumption allows for these latter three quantities to be set to zero in (27b), (27c), and (27d) when deriving (30) without altering the final result.

Next, we write the magnetic field fluctuations $\widetilde{\delta \boldsymbol{B}}_{\boldsymbol{k}}(s)$ and the temperature fluctuations $\widetilde{\delta T}_{\boldsymbol{k}}(s)$ in terms of velocity field fluctuations $\widetilde{\delta \boldsymbol{u}}_{\boldsymbol{k}}(s)$, using (27c) and (27d), respectively:

$$\widetilde{\delta \boldsymbol{B}}_{\boldsymbol{k}}(s) = \frac{i(\boldsymbol{k}\cdot\boldsymbol{B}_0)\widetilde{\delta \boldsymbol{u}}_{\boldsymbol{k}}(s) - i[\boldsymbol{k}\cdot\widetilde{\delta \boldsymbol{u}}_{\boldsymbol{k}}(s)]\boldsymbol{B}_0}{s + \eta_0 k^2}, \tag{B1a}$$

$$\widetilde{\delta T}_{\boldsymbol{k}}(s) = -\frac{i(\gamma_0 - 1)\boldsymbol{k}\cdot\widetilde{\delta \boldsymbol{u}}_{\boldsymbol{k}}(s)}{\alpha_{T0}(s + \gamma_0\chi_0 k^2)}. \tag{B1b}$$

We then solve for $\delta\widetilde{\boldsymbol{u}}_{\boldsymbol{k}}(s)\cdot\boldsymbol{B}_0$ in terms of $\widetilde{\delta\rho}_{\boldsymbol{k}}(s)$ and $i\rho_0\boldsymbol{k}\cdot\delta\widetilde{\boldsymbol{u}}_{\boldsymbol{k}}(s)$, by taking the scalar product of (27b) with $\boldsymbol{B}_0$, and substituting (B1a) and (B1b). This gives

$$\delta\widetilde{\boldsymbol{u}}_{\boldsymbol{k}}(s)\cdot\boldsymbol{B}_0 = -\frac{ic_{s0}^2(\boldsymbol{k}\cdot\boldsymbol{B}_0)}{\mu_0\gamma_0(\rho_0 s+\zeta_{s0}k^2)}\widetilde{\delta\rho}_{\boldsymbol{k}}(s) + \frac{i(\boldsymbol{k}\cdot\boldsymbol{B}_0)}{\mu_0(\rho_0 s+\zeta_{s0}k^2)}\left[\frac{(\gamma_0-1)c_{s0}^2}{\gamma_0(s+\gamma_0\chi_0k^2)}+\nu_{c0}\right]i\rho_0\boldsymbol{k}\cdot\delta\widetilde{\boldsymbol{u}}_{\boldsymbol{k}}(s). \tag{B2}$$

We can subsequently evaluate $i\rho_0\boldsymbol{k}\cdot\delta\widetilde{\boldsymbol{u}}_{\boldsymbol{k}}(s)$ in terms of $\widetilde{\delta\rho}_{\boldsymbol{k}}(s)$ alone, using the scalar product of Eq. (27b) and $i\boldsymbol{k}$, as well as substituting in (B1a), (B1b), and (B2):

$$\begin{aligned} is\rho_0\boldsymbol{k}\cdot\delta\widetilde{\boldsymbol{u}}_{\boldsymbol{k}}(s) = {}& \left[\frac{k^2c_{s0}^2}{\gamma_0}+\frac{k^2c_{s0}^2(\boldsymbol{k}\cdot\boldsymbol{B}_0)^2}{\mu_0\gamma_0(\rho_0 s+\zeta_{s0}k^2)(s+\gamma_0\chi_0k^2)}\right]\widetilde{\delta\rho}_{\boldsymbol{k}}(s) - \left\{\frac{(\gamma_0-1)k^4c_{s0}^2}{\gamma_0(s+\gamma_0\chi_0k^2)}+\nu_{l0}k^2+\frac{k^2B_0^2}{\mu_0\rho_0(s+\eta_0k^2)}\right. \\ & \left.+\frac{k^2(\boldsymbol{k}\cdot\boldsymbol{B}_0)^2}{\mu_0\rho_0(s+\eta_0k^2)(\rho_0 s+\zeta_{s0}k^2)}\left[\frac{(\gamma_0-1)c_{s0}^2}{\gamma_0(s+\gamma_0\chi_0k^2)}+\nu_{c0}\right]\right\}i\rho_0\boldsymbol{k}\cdot\delta\widetilde{\boldsymbol{u}}_{\boldsymbol{k}}(s). \end{aligned} \tag{B3}$$

This can be rearranged to give

$$i\rho_0\boldsymbol{k}\cdot\delta\widetilde{\boldsymbol{u}}_{\boldsymbol{k}}(s) = \left[\frac{Q(k,s)}{P(k,s)}-s\right]\widetilde{\delta\rho}_{\boldsymbol{k}}(s), \tag{B4}$$

where functions $P(k,s)$ and $Q(k,s)$ are defined by Eqs. (31a) and (31b) in the main text. Finally, we substitute (B4) into (27a) and solve for $\widetilde{\delta\rho}_{\boldsymbol{k}}(s)$ in terms of $\delta\rho_{\boldsymbol{k}}(0)$:

$$\widetilde{\delta\rho}_{\boldsymbol{k}}(s) = \frac{P(k,s)}{Q(k,s)}\delta\rho_{\boldsymbol{k}}(0). \tag{B5}$$

The density autocorrelation function (30) then follows immediately.

APPENDIX C: ANALYTIC CALCULATIONS OF THE DYNAMIC STRUCTURE FACTOR

In this Appendix, we outline the technique used to derive analytic expressions for the dynamic structure factor in the limit of weak damping: that is, fluctuations for which assumptions (36) apply. In particular, the technique leads to expression (37) for the dynamic structure factor associated with parallel fluctuations, (39) for quasiperpendicular fluctuations, and (46) for oblique fluctuations in the presence of a small but finite magnetic field.

The technique in general proceeds as follows. First, following assumptions (36), we neglect all diffusive effects and then determine the (imaginary) values $s_* = i\omega_*$ of s for which density autocorrelation function (30) vanishes. Equivalently, these values s are the roots of polynomial $Q(k,s)$ for fixed k. Then, for each s_*, we calculate the density autocorrelation function for s in the neighborhood of s_* when diffusive effects are included—that is, $|s-s_*| \sim \chi_0k^2, \eta_0k^2, \nu_{s0}k^2, \nu_{l0}k^2 \ll |s_*|$. The resulting expression typically possesses the form

$$\frac{\langle\delta\rho_{\boldsymbol{k}}^*(0)\widetilde{\delta\rho}_{\boldsymbol{k}}(s)\rangle}{\langle\delta\rho_{\boldsymbol{k}}^*(0)\delta\rho_{\boldsymbol{k}}(0)\rangle} \approx \frac{\mathcal{A}_*}{s-i\omega_*+\Delta\omega_*}, \tag{C1}$$

for $\mathcal{A}_*$ some characteristic amplitude and $\Delta\omega_* \sim \chi_0k^2, \eta_0k^2, \nu_{s0}k^2, \nu_{l0}k^2$ some typical frequency spread. Then applying formula (28), we conclude that the dynamic structure factor near the peak frequency ω_* is approximately

$$\frac{S_{nn}(k,\omega)}{S_{nn}(k)} \approx \frac{2\Delta\omega_*\mathcal{A}_*}{(\omega-\omega_*)^2+(\Delta\omega_*)^2}. \tag{C2}$$

The total structure factor is simply the sum over all scattering peak frequencies.

We illustrate the approach in the case of quasiperpendicular fluctuations, on account of the novelty of the result. First neglecting all diffusive effects, we find

$$Q(k,s) \approx s\left(s^2+k^2c_{SW}^2\right)\left(s^2+k^2c_{FW}^2\right), \quad P(k,s) \approx -k^2c_{s0}^2\left(s^2+k^2v_A^2\cos^2\theta\right)\big/\gamma_0, \tag{C3}$$

where c_{SW} and c_{FW} are given in the main text. The roots are then

$$s_* = 0, \quad \pm ikc_{SW}, \quad \pm ikc_{FW}. \tag{C4}$$

We then determine the density autocorrelation function in the neighborhood of each of these roots in turn. The numerator is $P(k,s_*) \neq 0$ in each case.

(i) $\underline{s_* = 0}$: Let $s = \delta s \sim \chi_0k^2, \eta_0k^2, \nu_{s0}k^2, \nu_{l0}k^2$. Then $Q(k,s) \approx k^4c_{s0}^2v_A^2\cos^2\theta\,(\delta s+\chi_0k^2)$, and so

$$\frac{\langle\delta\rho_{\boldsymbol{k}}^*(0)\widetilde{\delta\rho}_{\boldsymbol{k}}(s)\rangle}{\langle\delta\rho_{\boldsymbol{k}}^*(0)\delta\rho_{\boldsymbol{k}}(0)\rangle} \approx \frac{(\gamma_0-1)/\gamma_0}{s+\chi_0k^2}. \tag{C5}$$

(ii) $s_* = \pm ikc_{SW}$: Let $s = \pm ikc_{SW} + \delta s$, $\delta s \sim \chi_0 k^2, \eta_0 k^2, \nu_{s0} k^2, \nu_{l0} k^2$. Then $Q(k, s) \approx -2k^2 c_{SW}^2 c_{FW}^2 (\delta s + \Gamma_{SW})$, where Γ_{SW} is defined by (41a) in the main text. It follows that

$$\frac{\langle \delta\rho_{\boldsymbol{k}}^*(0)\widetilde{\delta\rho}_{\boldsymbol{k}}(s)\rangle}{\langle \delta\rho_{\boldsymbol{k}}^*(0)\delta\rho_{\boldsymbol{k}}(0)\rangle} \approx \frac{v_A^2/2\gamma_0 c_{FW}^2}{s \mp ikc_{SW} + \Gamma_{SW}}. \tag{C6}$$

(iii) $s_* = \pm ikc_{FW}$: Let $s = \pm ikc_{FW} + \delta s$, $\delta s \sim \chi_0 k^2, \eta_0 k^2, \nu_{s0} k^2, \nu_{l0} k^2$. Then $Q(k, s) \approx -2k^4 c_{FW}^4 (\delta s + \Gamma_{FW})$, where Γ_{FW} is also defined in the main text by (41b). We conclude that

$$\frac{\langle \delta\rho_{\boldsymbol{k}}^*(0)\widetilde{\delta\rho}_{\boldsymbol{k}}(s)\rangle}{\langle \delta\rho_{\boldsymbol{k}}^*(0)\delta\rho_{\boldsymbol{k}}(0)\rangle} \approx \frac{c_{s0}^2/2\gamma_0 c_{FW}^2}{s \mp ikc_{FW} + \Gamma_{FW}}. \tag{C7}$$

The dynamic structure function near each root is then given by (C2), with the total structure factor (39) simply being the sum of each of these terms.

[1] P. Meszaros, *High-Energy Radiation from Magnetized Neutron Stars* (University of Chicago Press, Chicago, 1992).
[2] R. M. Kulsrud, *Plasma Physics for Astrophysics* (Princeton University Press, Princeton, NJ, 2004).
[3] T. Guillot, Science **286**, 72 (1999).
[4] J. Lindl, Phys. Plasmas **2**, 3933 (1995).
[5] B. A. Remington, R. P. Drake, and D. D. Ryutov, Rev. Mod. Phys. **78**, 755 (2006).
[6] B. J. B. Crowley and G. Gregori, New J. Phys. **15**, 015014 (2013).
[7] D. E. Evans and J. Katzenstein, Rep. Prog. Phys. **32**, 207 (1969).
[8] H. Herold, Phys. Rev. D **19**, 2868 (1979).
[9] E. E. Salpeter, Phys. Rev. **122**, 1663 (1961).
[10] D. Froula, S. H. Glenzer, N. C. Luhmann, and J. Sheffield, *Plasma Scattering of Electromagnetic Radiation* (Academic Press, New York, 2010).
[11] S. I. Braginskii, in *Reviews of Plasma Physics*, edited by M. A. Leontovich (Consultants Bureau, New York, 1965), Vol. 1, p. 205.
[12] J. Colvin and J. Larsen, *Extreme Physics: Properties and Behavior of Matter at Extreme Conditions* (Cambridge University Press, Cambridge, 2013).
[13] J. Ventura, M. Soffel, H. Herold, and H. Ruder, Astron. Astrophys. **144**, 479 (1985).
[14] W. Nagel and J. Ventura, Astron. Astrophys. **118**, 66 (1983).
[15] J. Chihara, J. Phys.: Condens. Matter **12**, 231 (2000).
[16] G. Gregori, S. H. Glenzer, W. Rozmus, R. W. Lee, and O. L. Landen, Phys. Rev. E **67**, 026412 (2003).
[17] B. J. B. Crowley and G. Gregori, High Energy Dens. Phys. **13**, 55 (2014).
[18] J.-P. Hansen and I. R. McDonald, *Theory of Simple Liquids* (Academic Publications, Amsterdam, 2013).
[19] J. P. Boon and S. Yip, *Molecular Hydrodynamics* (Dover, New York, 1991).
[20] J. P. Mithen, J. Daligault, and G. Gregori, Phys. Rev. E **83**, 015401(R) (2011).
[21] I. R. McDonald, P. Vieillefosse, and J.-P. Hansen, Phys. Rev. Lett. **39**, 271 (1977).
[22] R. Schmidt, B. J. B. Crowley, J. P. Mithen, and G. Gregori, Phys. Rev. E **85**, 046408 (2012).
[23] J. E. Cross, P. Mabey, D. O. Gericke, and G. Gregori, Phys. Rev. E **93**, 033201 (2016).
[24] C. E. Max, Physics of Laser Fusion. Vol. I. Theory of the Coronal Plasma in Laser-Fusion Targets Rep. No. UCRL-53107, Lawrence Livermore National Laboratory, 1981.
[25] A. P. Kazantsev, Zh. Eksp. Teor. Fiz. **53**, 1806 (1968) [Sov. Phys. JETP **26**, 1031 (1968)].
[26] P. Tzeferacos, A. Rigby, A. F. A. Bott, A. R. Bell, R. Bingham, A. Casner, F. Cattaneo, E. M. Churazov, J. Emig, F. Fiuza, C. B. Forest, J. Foster, C. Graziani, J. Katz, M. Koenig, C.-K. Li, J. Meinecke, R. Petrasso, H.-S. Park, B. A. Remington *et al.*, Nat. Commun. **9**, 591 (2018).
[27] G. Gregori and D. O. Gericke, Phys. Plasmas **16**, 056306 (2009).
[28] J. D. Huba, *NRL Plasma Formulary* (Naval Research Laboratory, Washington DC, 1994).
[29] J. E. Cross, B. Reville, and G. Gregori, Astrophys. J. **795**, 59 (2014).
[30] T. Scopigno, G. Ruocco, and F. Sette, Rev. Mod. Phys. **77**, 881 (2005).
[31] U. Wagner, M. Tatarakis, A. Gopal, F. N. Beg, E. L. Clark, A. E. Dangor, R. G. Evans, M. G. Haines, S. P. D. Mangles, P. A. Norreys, M.-S. Wei, M. Zepf, and K. Krushelnick, Phys. Rev. E **70**, 026401 (2004).
[32] M. G. Haines, S. V. Lebedev, J. P. Chittenden, F. N. Beg, S. N. Bland, and A. E. Dangor, Phys. Plasma **7**, 1672 (2000).